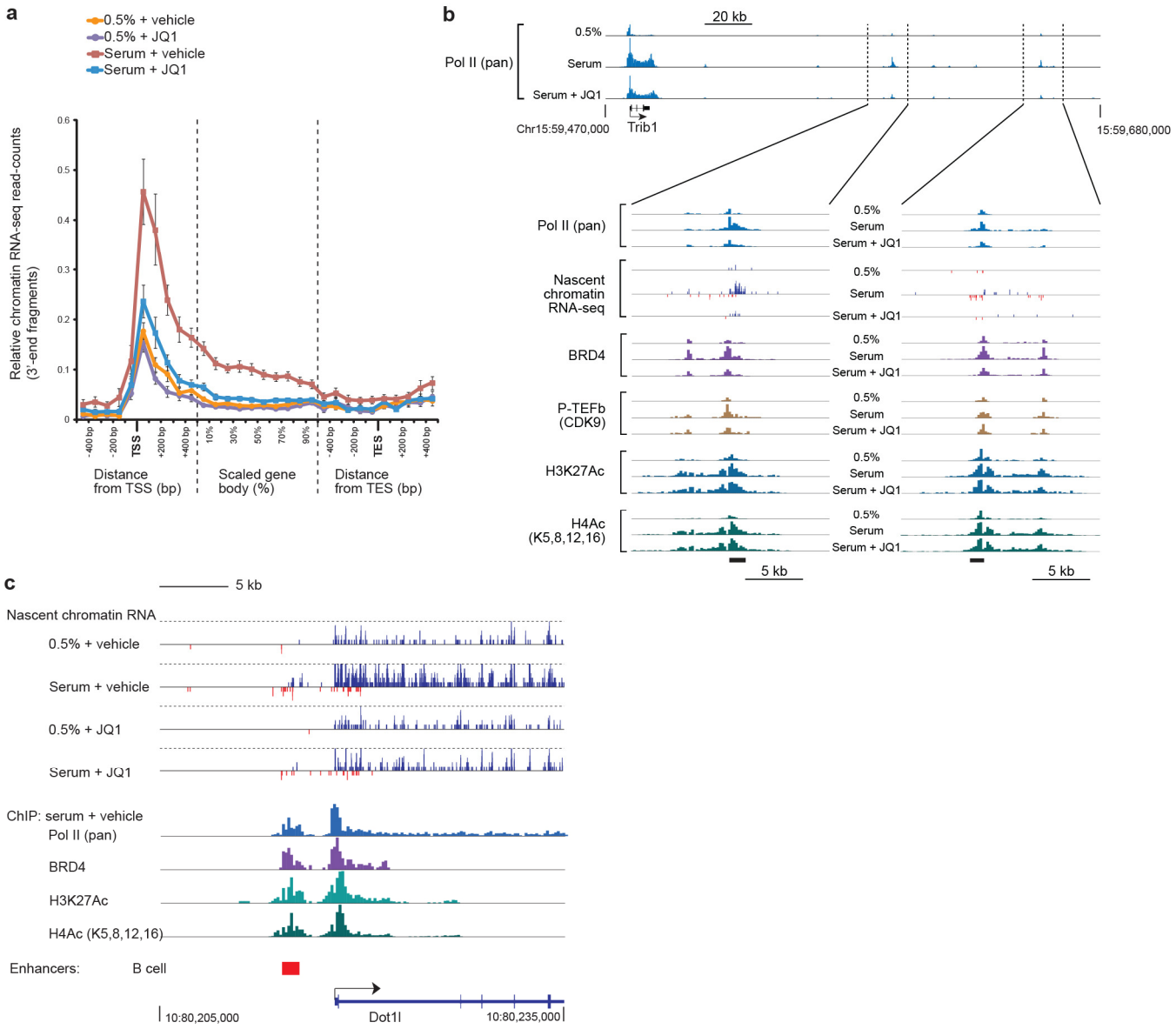

Supplementary Figure 1

The effects of BET inhibitor JQ1 on serum-induced nascent transcripts of protein-coding genes and flanking intergenic regions.

a, Metagene profiles of 66 genes larger than 2 kb, serum induction of which was inhibited by JQ1. (1) 0.5% + vehicle: cells were serum-starved, preincubated with vehicle, and left unstimulated. (2) 0.5% + JQ1: cells were serum-starved, preincubated with JQ1, and left unstimulated. (3) Serum + vehicle: cells were serum-starved, preincubated with vehicle, and then serum-stimulated. (4) 0.5% + JQ1: cells were serum-starved, preincubated with JQ1, and then serum-stimulated. For each gene, the sum of chromatin RNA-seq read-counts from 200 nt upstream of TSS to TES in cells treated with 0.5%+vehicle was calculated, and used to normalize read-counts in cells under all four experimental conditions. **b**, Genome browser views of the 3' enhancer regions of the Trib1 gene, characterized by chromatin RNA-seq, and the chromatin association of Pol II, BRD4, P-TEFb (CDK9), H3K27Ac, and H4Ac. For RNA-seq, sense- and antisense-strand signals are shown in upward and downward directions, respectively. Two regions exhibiting a prominent accumulation of ChIP signals as well as RNA-seq signals after serum stimulation are magnified in the lower part. JQ1 treatment mostly inhibited elongation of the non-coding transcripts without affecting acetylation of H3K27 and H4. Progression of Pol II and BRD4 were reduced by JQ1, but that of CDK9 was less affected. **c**, Genome browser views along the Dot1l gene and the upstream flanking region.

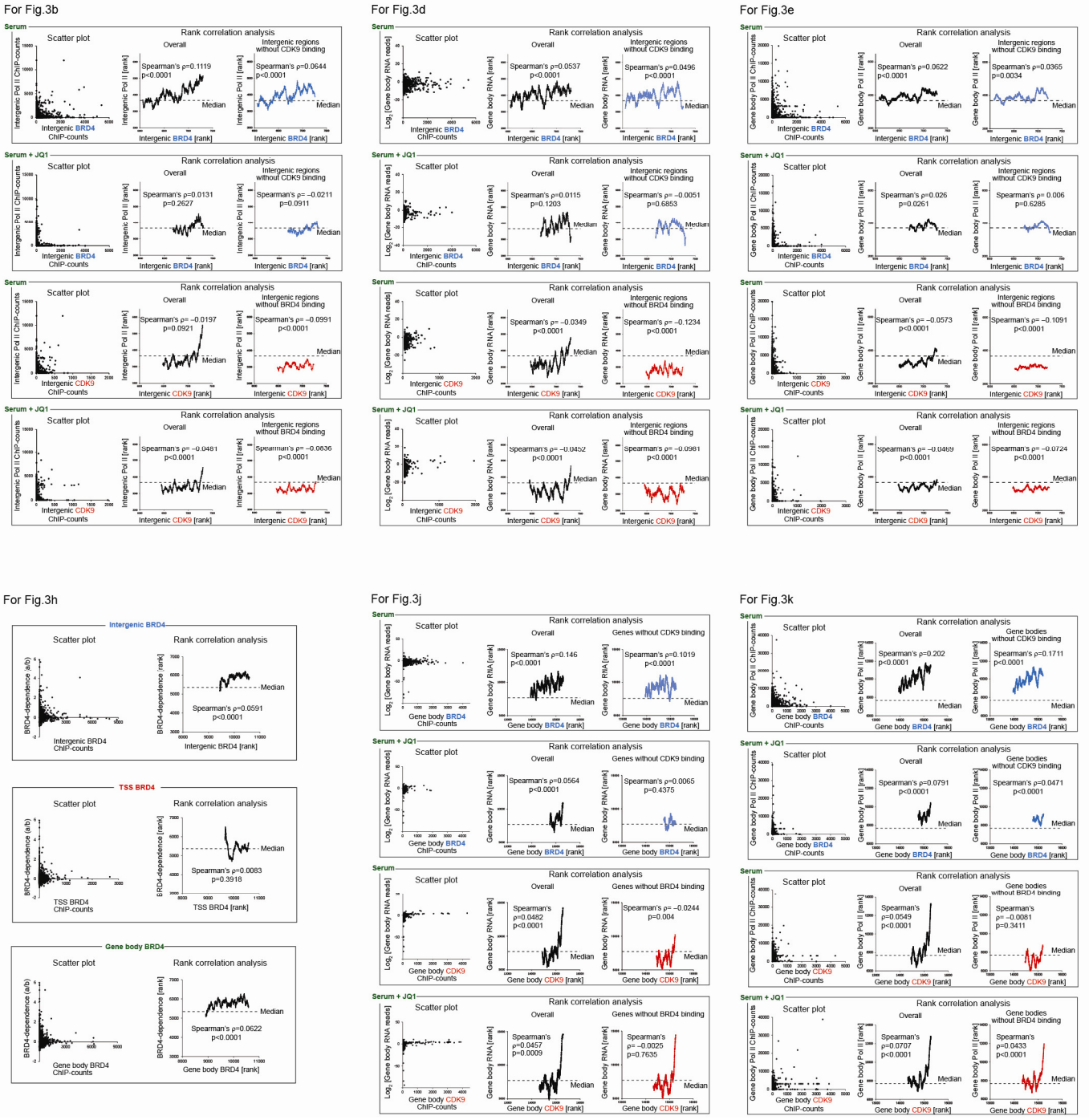

Supplementary Figure 2

Scatter plots and graphical displays of rank correlation.

Supplementary to Fig.3 panels b, d, e, h, j and k. For each panel, scatter plots of measured values, and correlation displays of ranks are shown. For the displays of rank correlation, moving averages were calculated according to the order of BRD4 or CDK9. The subset sizes were 50 for panels **b**, **d**, and **j**, 75 for panel **k**, 100 for panel **e**, and 200 for panel **h**. The median points of the ranks of the y axis are represented by the dotted lines. Spearman's ρ values and p-values are also shown. Note: these displays do not contain the lowest ranks on the x-axis (BRD4 or CDK9), because there were too many data points belonging to these ranks for the calculations.

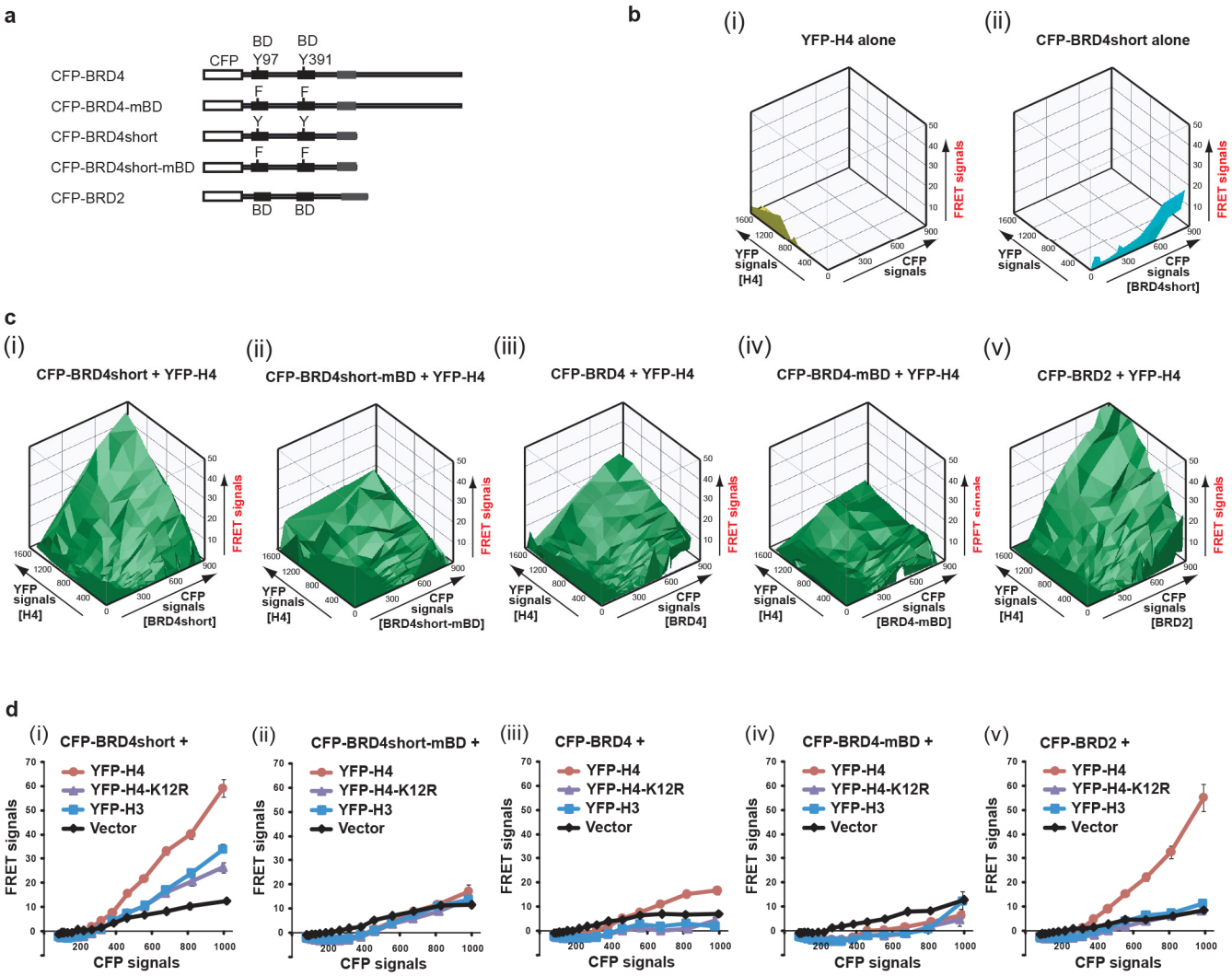

Supplementary Figure 3

Live-cell fluorescence resonance energy transfer (FRET) analysis of interactions between YFP-histones and CFP-BRD proteins.

a, Diagram of CFP-BRD proteins. **b**, Three-dimensional (3D) surface plots of FRET signals from HEK293T cells transfected with YFP-H4 alone (i) or CFP-BRD4short alone (ii). In flow cytometric measurements, spillover signals (e.g., false FRET signals due to spillover of CFP signals into the FRET detector channel) were digitally compensated so that YFP- or CFP-protein alone exhibited only marginal FRET signals. **c**, 3D surface plots displaying FRET signals covering wide ranges in CFP/YFP protein expression. HEK293T cells were transfected with YFP-H4 and CFP-BRD proteins as indicated. The same spillover-compensation matrix set in **b** was applied to all plots. **d**, Cells were transfected with expression plasmids for CFP-BRD proteins and YFP-histones or an empty vector in combinations as indicated. Data were collected using a fixed window set for similar levels of YFP-proteins, and FRET signals (means ± SEM) were plotted against CFP signals. For cells transfected with CFP-BRD plasmids and an empty vector, all data were collected.

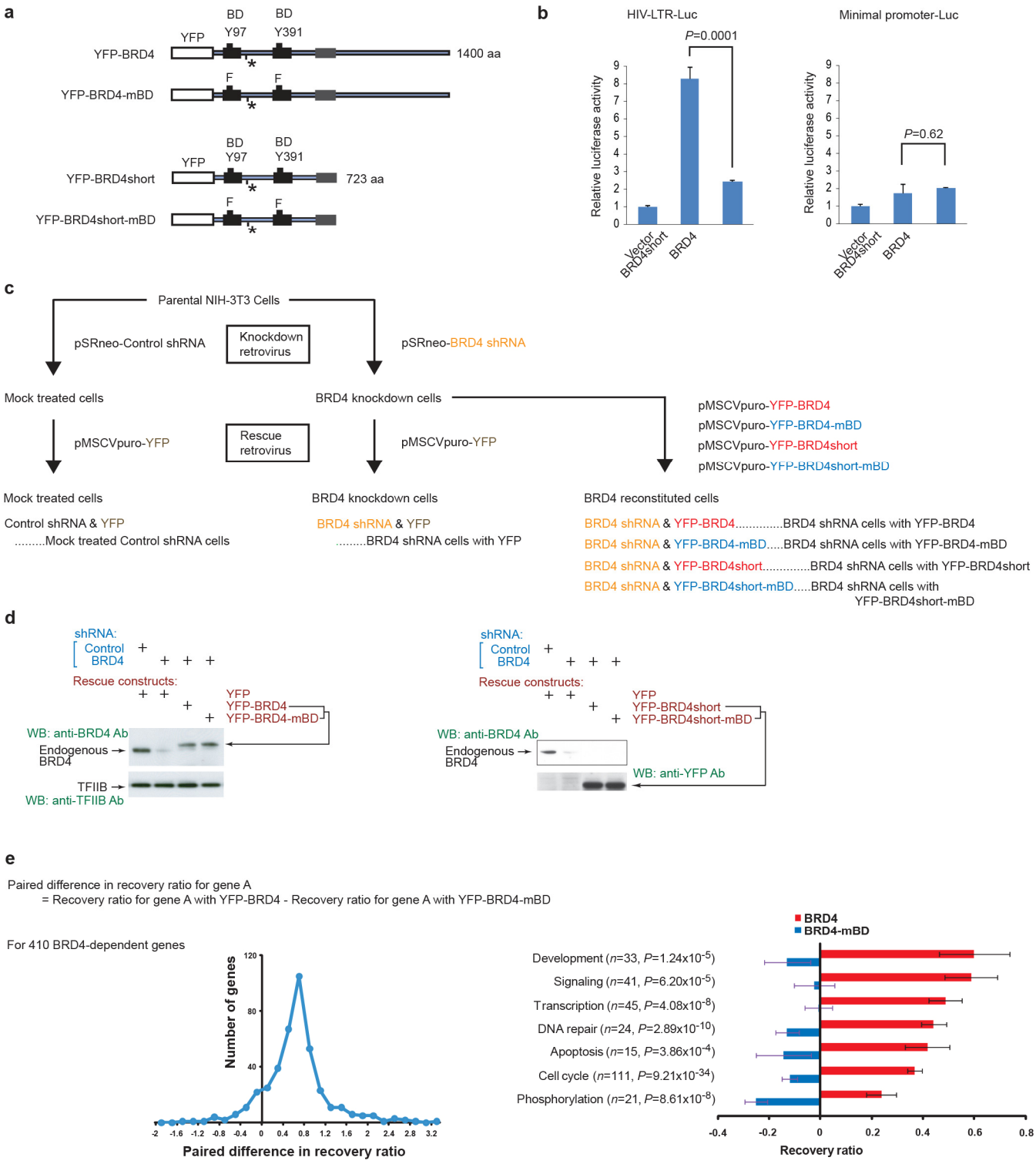

Supplementary Figure 4

BRD4 knockdown and reconstitution system.

a, Diagram of YFP-BRD4, YFP-BRD4-mBD, and their short forms. These BRD4 constructs contain nucleotide substitutions around the target site of BRD4 shRNA (marked by an asterisk) so that they are resistant to BRD4 shRNA while keeping the amino-acid coding

unchanged. **b**, Transient transcription reporter assays using HIV-LTR-Luc and minP-Luc (minimal promoter Luc) luciferase reporters. HIV-LTR-Luc is sensitive to P-TEFb activity, while minP-Luc is not. Of note, low levels of P-TEFb-independent luciferase activities were observed both with BRD4 and BRD4short on minP-Luc, which were comparable with those observed with BRD4short on HIV-LTR-Luc. **c**, Work flow to establish cells stably expressing YFP-BRD4 or YFP-BRD4-mBD (or their short forms) in place of endogenous BRD4. NIH3T3 cells were sequentially infected with shRNA retrovirus and YFP-BRD4 expressing retrovirus as shown. The transduced cells were selected with G418 and puromycin. **d**, Left panel: immunoblot with anti-BRD4 antibody. The positions of YFP-tagged BRD4 proteins and endogenous BRD4 are shown. Right panel: immunoblot with anti-BRD4 antibody for endogenous BRD4, and with anti-YFP (GFP) antibody for YFP-BRD4short proteins. **e**, Microarray gene expression analysis of the recovery of BRD4-dependent genes after BRD4 shRNA-mediated knockdown. Paired differences in the recovery ratios (RRs) of 410 BRD4 target genes are binned and plotted as in Fig.3g. In the right, BRD4 target genes are classified by gene ontology. In parenthesis shown are the numbers of genes in each group and P values of paired t test on the RR compared between the YFP-BRD4 and YFP-BRD4-mBD reconstituted cells, all of which are statistically significant. Bars represent means ± s.e.m. of the RRs.

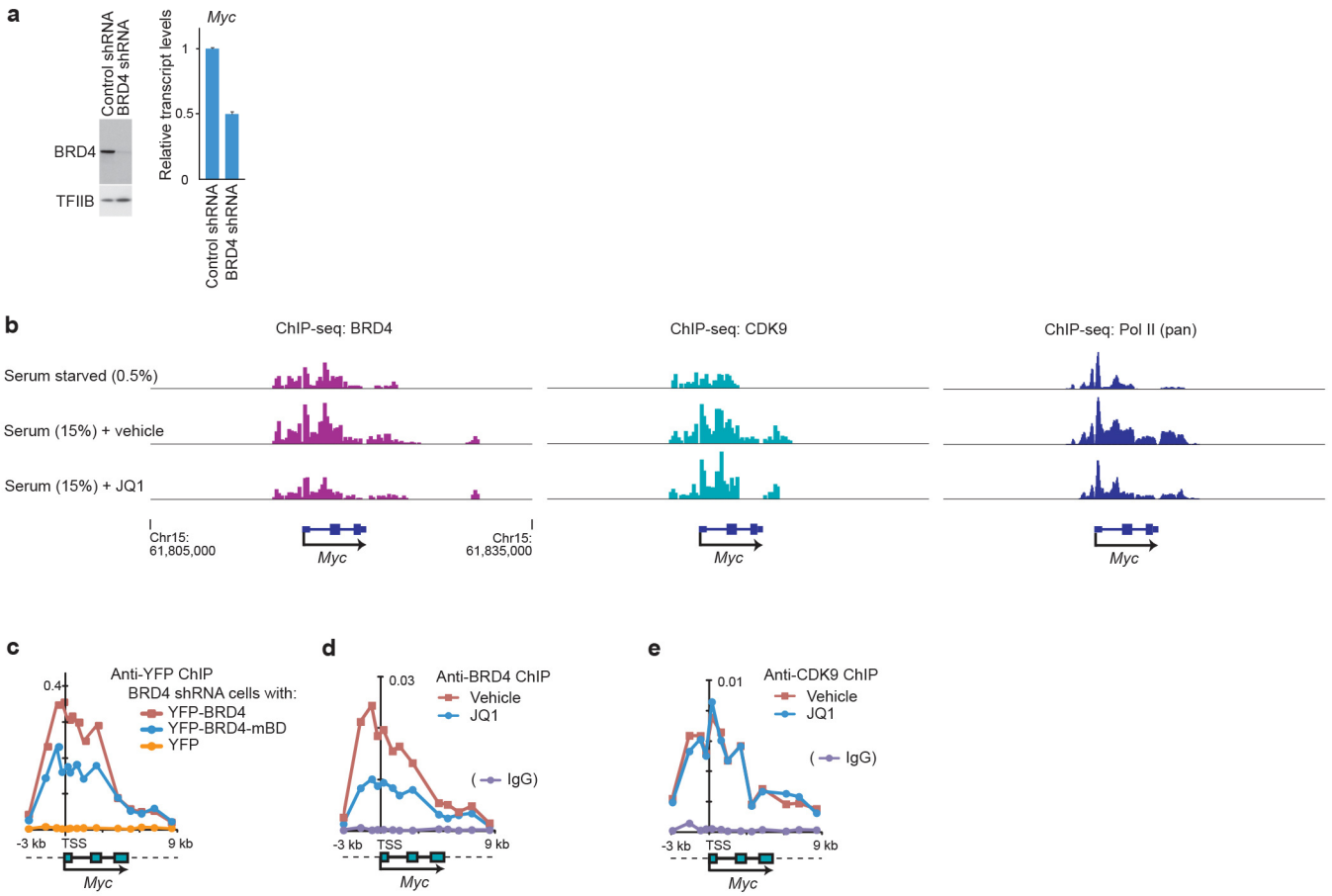

Supplementary Figure 5

ChIP assays to detect binding of BRD4, CDK9 and Pol II over the *Myc* gene loci.

a, Effects of BRD4 knockdown by BRD4 shRNA on BRD4 protein and Myc transcript levels in NIH3T3 cells. **b**, Genome browser views of ChIP-seq signals for BRD4, CDK9 and Pol II (pan) along the Myc gene in NIH3T3 cells treated as indicated on the left. **c**, BRD4 knockdown cells were reconstituted with YFP-BRD4, YFP-BRD4-mBD or YFP alone. ChIP-qPCR assays using anti-YFP (GFP) antibody demonstrate binding of YFP-BRD4 or YFP-BRD4-mBD on the *Myc* gene locus. Signals relative to input DNA (y-axis) are plotted against positions of PCR primers (x-axis: covering the same region as the *Myc* gene locus shown at the bottom). In the gene locus diagram, dotted lines represent the upstream and downstream regions flanking the *Myc* gene. Background signals were assessed with cells expressing YFP alone. **(d, e)** ChIP-qPCR assays demonstrating binding of BRD4 (**d**) and CDK9 (**e**) on the *Myc* gene locus (shown at the bottom) in cells treated with JQ1 (1 μM, 2 h) or vehicle (DMSO). Background signals were assessed using normal rabbit IgG.

a

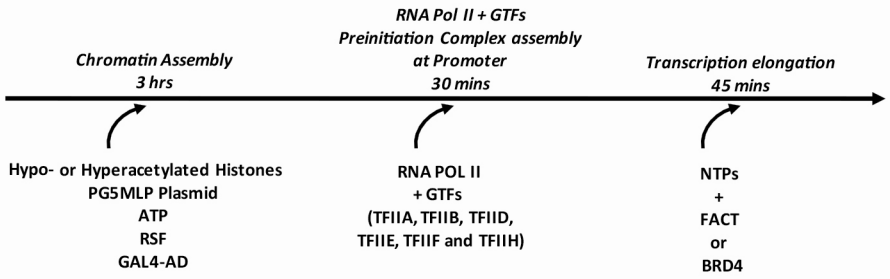

b Relative quantification of histone H3 modifications by quantitative mass spectrometry in hypo-acetylated and hyper-acetylated nucleosomes.

Peptide	Modifications	Hypo-acetylated 1	Hypo-acetylated 2	Hypo-acetylated Avg	Hyper-acetylated 1	Hyper-acetylated 2	Hyper-acetylated Avg.
TKQTAR	H3K4un	79.61%	80.00%	79.80%	67.89%	67.44%	67.67%
	H3K4me1	20.36%	19.99%	20.17%	32.06%	32.49%	32.28%
	H3K4me2	0.01%	0.01%	0.01%	0.06%	0.06%	0.06%
KSTGGKAPR	H3K9unK14un	28.32%	29.71%	29.01%	14.29%	14.14%	14.21%
	H3K9me1K14un	14.88%	15.00%	14.94%	6.84%	6.90%	6.87%
	H3K9me2K14un	25.25%	25.15%	25.20%	15.38%	14.96%	15.17%
	H3K9me3K14un	14.82%	13.92%	14.37%	11.43%	11.35%	11.39%
	H3K9acK14un	0.49%	4.03%	2.26%	1.67%	8.42%	5.04%
	H3K9unK14ac	5.90%	2.11%	4.01%	8.71%	1.65%	5.18%
	H3K9me1K14ac	7.39%	7.13%	7.26%	18.35%	19.56%	18.96%
	H3K9me2K14ac	1.92%	1.95%	1.94%	9.99%	9.75%	9.87%
	H3K9me3K14ac	0.77%	0.74%	0.76%	4.05%	4.07%	4.06%
	H3K9acK14ac	0.25%	0.26%	0.26%	9.29%	9.21%	9.25%
KQLATKAAR	H3K18unK23un	72.88%	72.68%	72.78%	33.21%	31.42%	32.32%
	H3K18unK23me1	0.11%	0.08%	0.09%	0.45%	0.25%	0.35%
	H3K18me1K23un	0.28%	0.32%	0.30%	0.01%	0.22%	0.11%
	H3K18acK23un	1.40%	0.64%	1.02%	1.09%	2.16%	1.62%
	H3K18unK23ac	24.39%	25.32%	24.85%	44.02%	44.20%	44.11%
	H3K18acK23ac	0.94%	0.96%	0.95%	21.23%	21.74%	21.49%
KSAPATGGVKKPHR	H3K27unK36un	9.23%	8.71%	8.97%	11.23%	11.85%	11.54%
	H3K27unK36me1	2.46%	3.11%	2.78%	1.83%	1.57%	1.70%
	H3K27me1K36un	12.64%	10.64%	11.64%	10.75%	10.77%	10.76%
	H3K27me2K36un	24.36%	25.23%	24.79%	28.04%	26.88%	27.46%
	H3K27unK36me2	4.38%	4.47%	4.43%	2.45%	2.65%	2.55%
	H3K27me3K36un	8.36%	8.73%	8.54%	10.82%	10.71%	10.77%
	H3K27acK36un	0.21%	0.19%	0.20%	0.93%	0.94%	0.93%
	H3K27me1K36me1	3.33%	3.05%	3.19%	2.13%	2.05%	2.09%
	H3K27me2K36me1	15.39%	15.58%	15.48%	13.26%	13.08%	13.17%
	H3K27me1K36me2	6.25%	6.34%	6.29%	5.90%	6.24%	6.07%
	H3K27me2K36me2	5.09%	5.32%	5.21%	4.45%	4.44%	4.44%
	H3K27me3K36me1	3.87%	4.04%	3.95%	3.67%	4.31%	3.99%
	H3K27me1K36me3	3.07%	3.13%	3.10%	3.29%	3.31%	3.30%
	H3K27me3K36me2	1.35%	1.43%	1.39%	1.22%	1.20%	1.21%
	H3K27me3K36me3	0.02%	0.02%	0.02%	0.02%	0.02%	0.02%
YQKSTELLIR	H3K56un	68.50%	68.30%	68.40%	90.75%	80.17%	85.46%
	H3K56ac	31.50%	31.70%	31.60%	9.25%	19.83%	14.54%
EIAQDFKTDLR	H3K79un	81.09%	83.28%	82.18%	82.13%	81.73%	81.93%
	H3K79me1	12.24%	10.10%	11.17%	12.93%	13.34%	13.14%
	H3K79me2	6.68%	6.62%	6.65%	4.94%	4.92%	4.93%

Supplementary Figure 6

In vitro transcription assays on chromatin templates.

a, Diagram showing protocol for the *in vitro* transcription assays on chromatin templates. *In vitro* transcription elongation assays were performed on a hypo-acetylated or hyper-acetylated chromatin pG5MLP template, using recombinant FACT or BRD4; together with general transcription factors (GTFs) and RNA polymerase II. **b**, Relative quantification of histone H3 modifications by quantitative mass spectrometry in hypo-acetylated and hyper-acetylated nucleosomes. Results of two independent measurements are shown.

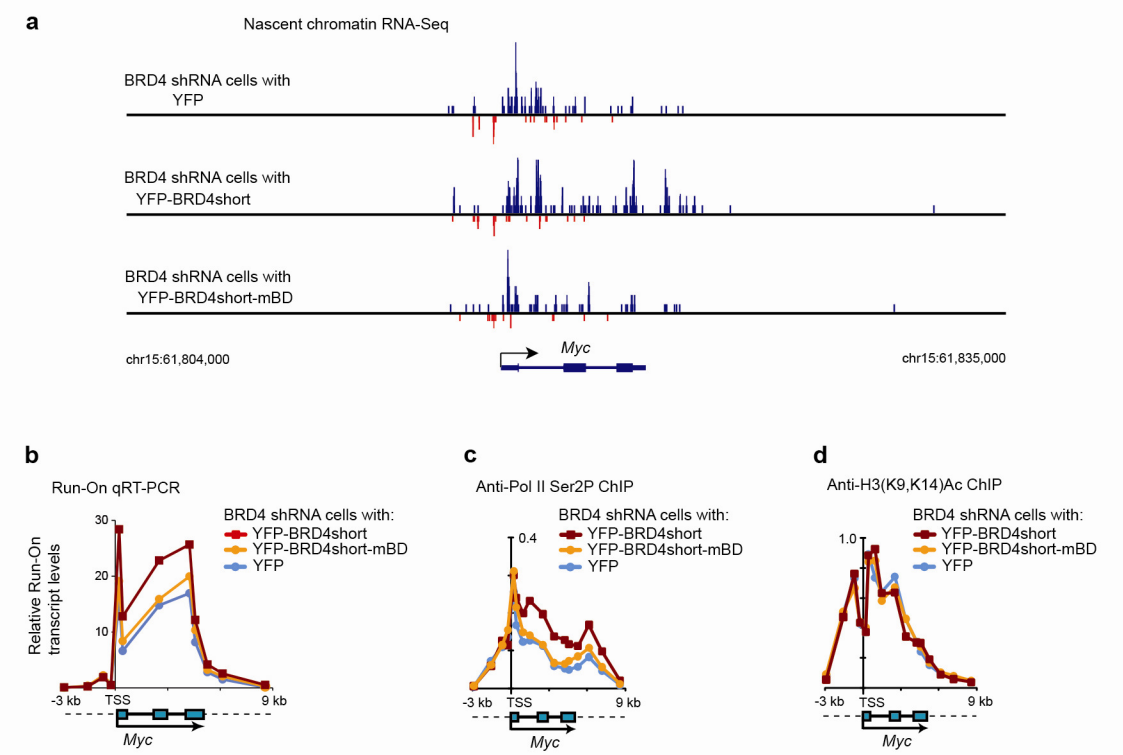

Supplementary Figure 7

BRD4short facilitates progression of Pol II and transcript elongation on the *Myc* gene by binding to acetylated histones through bromodomains *in vivo*.

a, Genome browser views of nascent transcript progression across the Myc gene locus, measured by chromatin RNA-seq analysis. **b**, BrU-labeled nuclear run-on RNA signals (measured by qRT-PCR) aligned along the *Myc* gene locus. Nuclei were isolated from BRD4 knockdown cells reconstituted with YFP-BRD4short, YFP-BRD4short-mBD or YFP alone, and subjected to a nuclear run-on reaction in the presence of 1% sarkosyl, and BrUTP, ATP, CTP, and GTP. The run-on RNAs labeled with BrU were fragmented, immunoprecipitated with anti-BrdU antibody, and analyzed by qRT-PCR using *Myc* locus specific primers. PCR efficiency was normalized with genomic DNA, and relative values of the run-on transcript signals are plotted against genomic positions corresponding to the PCR primers. (**c, d**) ChIP-qPCR assays for Ser2 phosphorylated Pol II (**c**) or K9/K14 acetylated H3 (**d**) along the Myc gene locus.

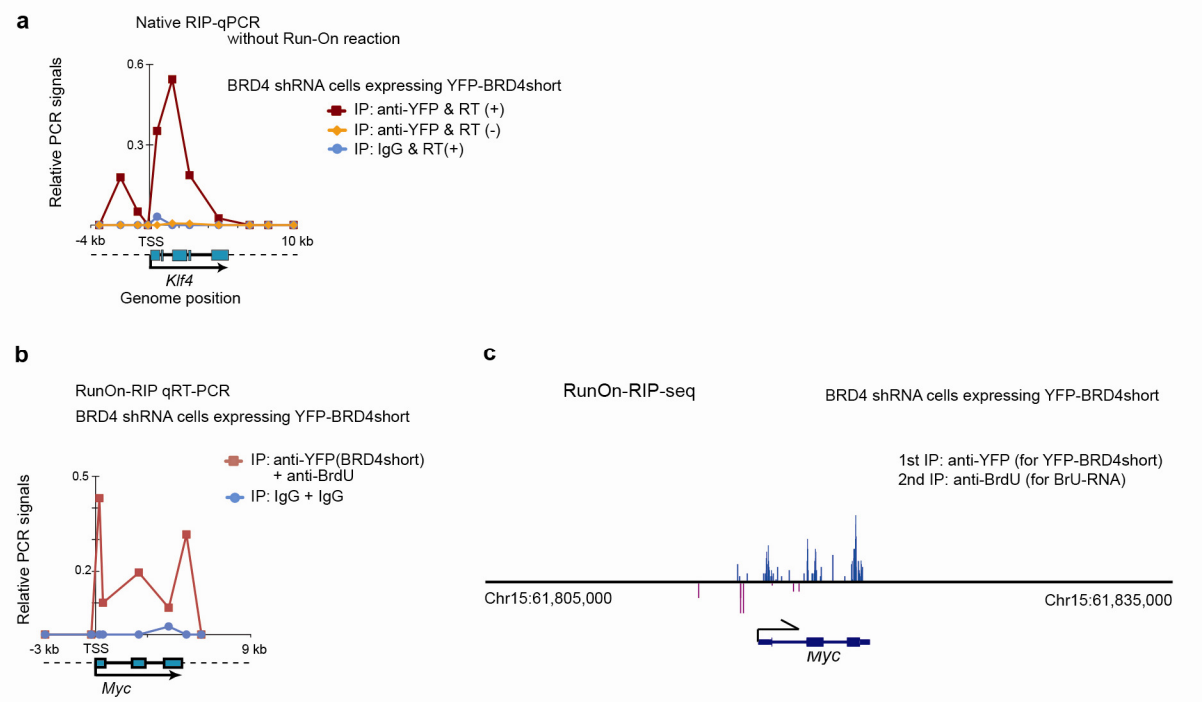

Supplementary Figure 8

BRD4 is associated with Pol II elongation complexes *in* vivo.

a, Validation of native RIP (RNA-Immunoprecipitation). Native nuclear complexes containing YFP-BRD4short and RNA were released by DNaseI digestion, and immunoprecipitated with anti-YFP antibody (for BRD4short) or control IgG, followed by extraction of co-precipitated RNA. Quantitative PCR using Klf4 specific primers was performed with or without reverse transcription (RT). **b**, Quantitative RT-PCR analysis of the RunOn-RIP signals along the Myc gene locus. Background signals were assessed using normal rabbit IgG. **c**, Genome browser view of RunOn-RIP-seq reads around the *Myc* gene locus, representing the actively elongating front of transcripts that was associated with YFP-BRD4short.

Supplementary Data Set1

Figure 5a

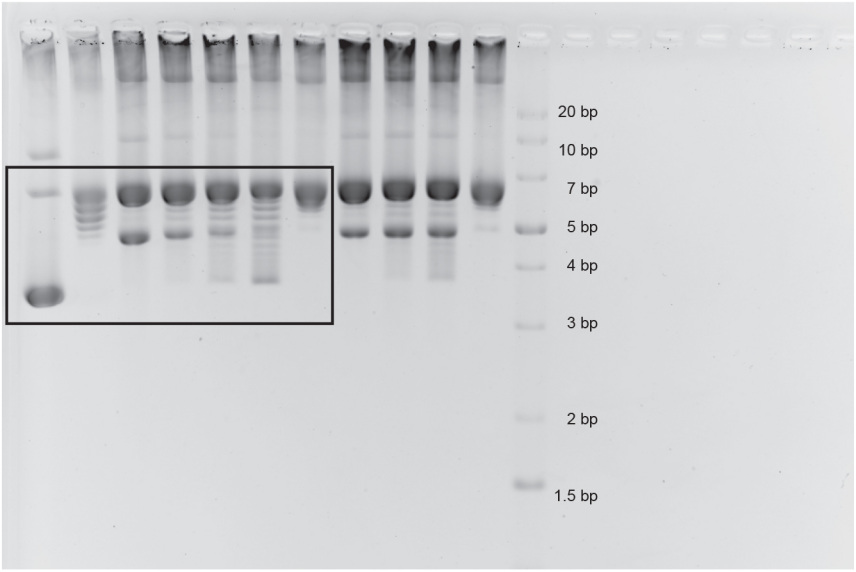

Figure 5d